Q_{EC}-values of the Superallowed β-Emitters ^{10}C, ^{34}Ar, ^{38}Ca and ^{46}V

T. Eronen,[1,*] D. Gorelov,[1] J. Hakala,[1] J. C. Hardy,[2] A. Jokinen,[1] A. Kankainen,[1] I. D. Moore,[1] H. Penttilä,[1] M. Reponen,[1] J. Rissanen,[1] A. Saastamoinen,[1] and J. Äystö[1]

[1]*Department of Physics, P.O. Box 35 (YFL), FI-40014 University of Jyväskylä, Finland*
[2]*Cyclotron Institute, Texas A&M University, College Station, Texas 77843, USA*

(Dated: January 21, 2011)

The Q_{EC} values of the superallowed β^+-emitters ^{10}C, ^{34}Ar, ^{38}Ca and ^{46}V have been measured with a Penning-trap mass spectrometer to be 3648.12(8), 6061.83(8), 6612.12(7) and 7052.44(10) keV, respectively. All four values are substantially improved in precision over previous results.

PACS numbers: 21.10.Dr, 23.40.Bw, 27.20.+n, 27.30.+t, 27.40.+z,

I. INTRODUCTION

Superallowed $0^+ \rightarrow 0^+$ β decay between $T = 1$ nuclear analog states plays an important role in several fundamental tests of the three-generation Standard Model. It tests the Conservation of the Vector Current (CVC), probes for the presence of scalar currents, and is a key contributor to the most demanding currently available test of the unitarity of the Cabibbo-Kobayashi-Maskawa (CKM) matrix [1]. For these and other reasons, it has been a subject of continuous and often intense study for six decades. The most important features of these superallowed transitions, and the ones that make them so attractive, are that their measured ft values are nearly independent of nuclear-structure ambiguities and that they depend uniquely on the vector (and scalar, if it exists) part of the weak interaction.

To date, the measured ft values for transitions from ten different nuclei are known to ∼0.1% precision, and three more are known to between 0.1% and 0.3%. An analysis of these ft values [2] recently demonstrated that the vector coupling constant, G_V, has the same value for all thirteen transitions to within ±0.013%, thus confirming a key part of the CVC hypothesis; and it sets an upper limit on a possible scalar current at 0.2% of the vector current. With both these outcomes established, the results could then be used to extract a value for V_{ud}, the up-down element of the CKM matrix, with which the top-row unitarity test of that matrix yielded the result 0.9999(6) [1]. This is in remarkable agreement with the Standard Model, and the tight uncertainty significantly limits the scope for any new physics beyond the model. Further tightening of the uncertainty would, of course, increase the impact of this result even more.

Neglecting for now the possibility of any scalar current, we can relate the ft value for a superallowed $0^+ \rightarrow 0^+$ transition directly to the vector coupling constant, G_V by the following equation [2]:

$$\mathcal{F}t \equiv ft(1+\delta'_R)(1+\delta_{NS}-\delta_C) = \frac{K}{2G_V^2(1+\Delta_V^R)} \ , \quad (1)$$

where $\mathcal{F}t$ is defined to be the "corrected" ft value and $K/(\hbar c)^6 = 2\pi^3\hbar \ln 2/(m_e c^2)^5 = 8120.2787(11) \times 10^{-10}$ GeV^{-4}s. There are four small correction terms: δ_C is the isospin-symmetry-breaking correction; Δ_V^R is the transition-independent part of the radiative correction; and the terms δ'_R and δ_{NS} comprise the transition-dependent part of the radiative correction, the former being a function only of the maximum positron energy and the atomic number, Z, of the daughter nucleus, while the latter, like δ_C, depends in its evaluation on the details of nuclear structure. The two structure-dependent terms δ_C and δ_{NS}, which appear in Eq. 1 as a difference, together contribute ≤1% to most $\mathcal{F}t$ values [3]. Even so, at the current level of experimental precision, their theoretical uncertainties contribute significantly to the final $\mathcal{F}t$-value uncertainties.

Experiments can help to reduce these theoretical uncertainties. A method has recently been proposed [4], by which the structure-dependent corrections can be validated. The calculated corrections change considerably from transition to transition, and the validation entails a comparison of these changes against the experimental changes from transition to transition in the uncorrected ft values. In essence, validation depends on whether the calculated corrections produce a result consistent with CVC. The effectiveness of this validation process depends directly on the experimental precision of the ft values.

The ft value that characterizes any β-transition depends on three measured quantities: the total transition energy, Q_{EC}; the half-life, $t_{1/2}$, of the parent state; and the branching ratio, R, for the particular transition of interest. The Q_{EC}-value is required to determine the statistical rate function, f, while the half-life and branching ratio combine to yield the partial half-life, t. It is important to recognize, though, that f varies approximately with the fifth power of Q_{EC}: If the fractional uncertainty in the measured Q_{EC} value is 1×10^{-4}, the corresponding uncertainty in f is $\sim5\times10^{-4}$. Thus, the precision required for Q_{EC}-value measurements is substantially higher than that required for half-lives and branching ratios.

We report here Q_{EC}-value results for ^{10}C, ^{34}Ar, ^{38}Ca and ^{46}V with fractional uncertainties in the range (1-5)$\times10^{-5}$, substantially better than any previous mea-

*Electronic address: tommi.eronen@phys.jyu.fi

surements for these transitions, and low enough that, with improvements in their half-lives and branching ratios, the uncertainties in these $\mathcal{F}t$ values could in principal be reduced to $\sim 1 \times 10^{-4}$, a factor of five to ten below the uncertainties of the best-known cases today.

The superallowed decay of ^{10}C is a particularly interesting case. If scalar currents exist, they would lead to a discrepancy between the $\mathcal{F}t$ values for the transitions in light nuclei and the average $\mathcal{F}t$ value for the heavier nuclei (see Fig. 7 in Ref. [2]). In particular, the decays of ^{10}C and ^{14}O are the most sensitive to the presence of a scalar current. Improved experimental precision for these two cases would have a significant impact on the search for a scalar current. If it were to be found, of course, that would constitute new physics beyond the standard model. Our ^{10}C measurement reported here is the first step along this path.

II. EXPERIMENTAL METHOD

The targets, proton beam energies, and reactions we employed in these measurements are listed in Table I.

The experiments were carried out with the JYFLTRAP Penning-trap mass spectrometer at the University of Jyväskylä, Finland [5]. The ions of interest were produced from fusion-evaporation reactions induced by protons from the K130 cyclotron, with the reaction products being collected and separated by the IGISOL technique [6], which is both universal and fast, enabling extraction of beams of any element within less than 100 ms. The recoiling nuclei are primarily slowed down in the target itself but are ultimately thermalized in a helium-filled stopping volume [7]. The ions flow with helium out from the gas cell and into a sextupole ion guide [8], after which they are electrostatically accelerated to an energy of $30q$ keV. These energetic ions are then separated with a 55° dipole magnet, which has a mass resolving power R ($\equiv M/\Delta M$) of about 500,

TABLE I: The proton beam energies and target combinations used in these measurements. Where applicable, the percentage of isotopic enrichment is given in parenthesis. Only the ^{46}Ti target was self supporting; all others were evaporated onto thin nickel foil. In all cases, the target thickness was a few mg/cm^2.

Target	E_{protons}	Reaction	Product(s)
^{10}B ($\approx$ 90%)	12 MeV	^{10}B(p,n)	^{10}C
		^{10}B(p,p)	^{10}B
KCl	35 MeV	^{35}Cl(p,2n)	^{34}Ar
		^{35}Cl(p,pn)	^{34}Cl+^{34}Cl^m
		^{35}Cl(p,2p)	^{34}S
KCl	35 MeV	^{39}K(p,2n)	^{38}Ca
		^{39}K(p,pn)	^{38}K+^{38}K^m
		^{39}K(p,2p)	^{38}Ar
^{46}Ti (> 90%)	20 MeV	^{46}Ti(p,n)	^{46}V

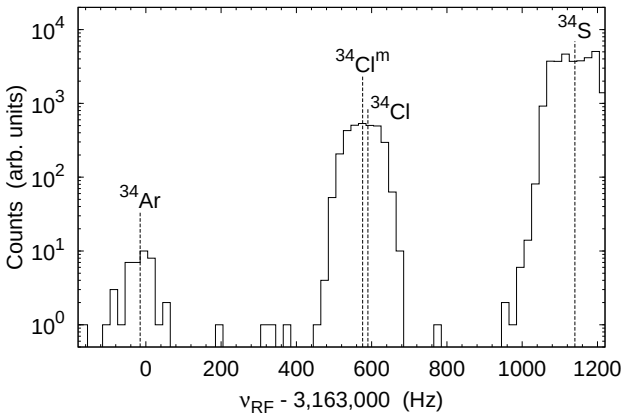

FIG. 1: Quadrupole frequency scan of the purification trap. The trap was tuned in this case to have a mass resolving power R of about 30,000, which is enough to separate isobars but not the isomeric states of ^{34}Cl.

and injected into a radiofrequency quadrupole (RFQ) structure for ion-beam cooling and bunching [9]. Finally, each bunch is released to the JYFLTRAP Penning-trap setup where the ions' masses are measured with the time-of-flight ion-cyclotron-resonance (TOF-ICR) technique [10].

A. Ion preparation

Ideally only one ion at a time is needed for a measurement, but in practice a few ions are usually used. However, the ions of interest typically comprise less than 1% of the mass-separated beam from IGISOL, so to have, for example, a few ^{34}Ar ions in a bunch, we have to collect 2-3 orders-of-magnitude more ions — mostly ^{34}Cl and ^{34}S — in the RFQ buncher. Once a large enough bunch has been collected, it is sent to the first of the two Penning traps that comprise the JYFLTRAP setup. This first trap contains helium buffer gas and serves to purify the sample. In it, the ions of interest are spatially separated with the sideband cooling technique [11]. After separation, the ions are extracted towards the second Penning trap, their path to that trap being via an electrode, in which there is a narrow central channel 2-mm in diameter. Only the centered ions of interest can pass through this channel, while the other ions hit the electrode. The transmitted ions are then captured in the second, precision Penning trap, which is operated in vacuum. There, the TOF-ICR mass measurement could in principal be initiated.

However, in the case of close-lying isomeric states purity is not yet assured. As shown in Fig. 1 for the mass-34 measurements, the purification process in the first Penning trap is sufficent to make clean bunches of ^{34}Ar, but it is not enough to separate ^{34}Cl from ^{34}Cl^m. The same problem occurs in the case of mass-38 as well. For

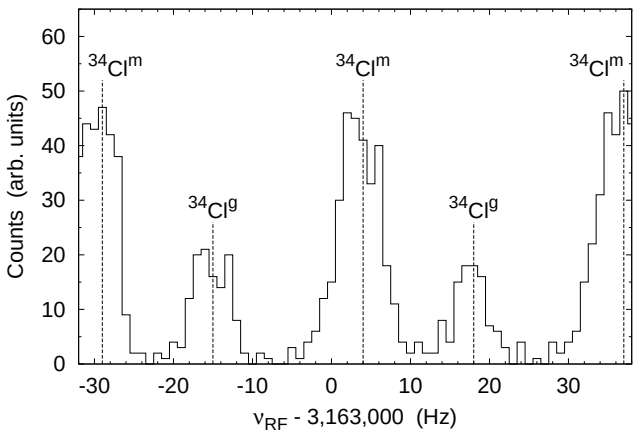

FIG. 2: Dipole frequency scan in the precision trap for bunches containing both ^{34}Cl and ^{34}Cl^m. With an excitation time-pattern of 10/20/10 ms (on/off/on) a mass resolving power $R \approx 5 \times 10^5$ was obtained. The two states of ^{34}Cl are cleanly separated.

these measurements we used the so-called Ramsey cleaning technique [12], in which a further purification is accomplished by use of a dipole rf electric field to drive the unwanted ions to large cyclotron orbits in the gas-free precision trap. The excitation pattern and duration are chosen so that, upon completion, ions in the unwanted state have a large orbit. The ions are then transferred back to the purification trap and, en route, the unwanted ions hit the electrode rather than passing through the narrow central channel. An example of a cleaning frequency scan is shown in Fig. 2.

Even with ions that did not require such high-precision cleaning, we chose to transfer them back from the precision trap to the purification trap. There the monoisomeric ion sample was recooled and recentered with the sideband cooling technique [11]. Only after this second purification step was the ion bunch sent to the precision trap for the TOF-ICR mass measurement. We found that this additional cooling step significantly improved the quality of the measured TOF-ICR resonances and thus improved our precision. The full ion preparation cycle is illustrated in Fig. 3.

B. TOF-ICR measurement

In these measurements the time-of-flight ion-cyclotron resonance (TOF-ICR) technique [10] has been applied not only in conventional square-wave mode [13] but also in time-separated (Ramsey-type) mode [14, 15]. The measurement procedure starts with a phase-locked dipole rf electric field used to increase slightly the magnetron orbit radius of the ions [16]. In measurements reported in this work, this excitation was applied for a single magnetron period of about 5.5 ms and with an amplitude of about 50 mV.

Following the dipole magnetron excitation, a quadrupole excitation was switched on to couple the two radial trap eigenmotions. The frequency of this quadrupole excitation was scanned over a range that included the sum of the two eigenfrequencies ν_c, which is also the cyclotron frequency of ions in the absence of any trapping electric fields: viz.

$$\nu_c = \nu_+ + \nu_- = \frac{1}{2\pi}\frac{q}{m}B, \qquad (2)$$

where ν_+ and ν_- are the frequencies of the two radial motions, commonly called the trap-modified cyclotron and magnetron frequencies, respectively; q/m is the charge-to-mass ratio of the ions and B is the magnetic field. The duration we could use for the excitation was limited not only by the half-life of the ions of interest, but also by ion-motion damping effects caused by residual gas present in the precision trap. These effects are much stronger with lighter ions. The excitation durations we used were between 200 ms and 400 ms.

After completion of the quadrupole excitation, the ions were released from the trap in the direction of a microchannel plate (MCP) detector. As ions travel through a region with high magnetic field gradient, their radial energy converts to axial velocity, so ions starting with more radial energy will gain more speed and thus arrive earlier at the detector than the ions that have not been resonantly excited. Since the energy content of the trap-modified cyclotron motion (ν_+) is of the order of several eV and the energy of the magnetron motion (ν_-) is only a few μeV, the resonantly excited ions can have as much as a factor of two shorter time-of-flight to the MCP detector than non-excited ions. Figure 4 shows a sample TOF-ICR curve for ^{34}Ar, in which the measured ion time-of-flight is plotted as a function of the quadrupole-excitation frequency over a 30 Hz range. In this case, the ion-motion excitation was accomplished by use of Ramsey's method of time-separated oscillatory fields.

Figure 4 also shows a fit to the experimental data. For the mass-34 measurement illustrated in the figure, and also for the mass-38 and mass-46 measurements, we took the shape of the Ramsey-type resonance from Ref. [14]. For the mass-10 measurements we could not use the Ramsey procedure (see Sec. III A for more details) and had to

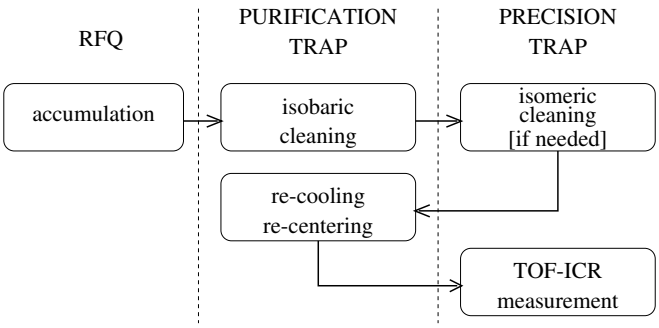

FIG. 3: The measurement cycle.

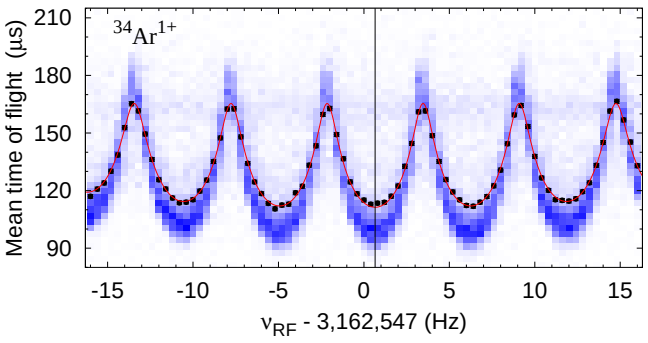

FIG. 4: (color online) A TOF-ICR curve measured for $^{34}Ar^{+}$ ions. An excitation time pattern of 25/150/25 ms (on/off/on) was used. The black circles (with error bars smaller than the points) are time-of-flight averages for each frequency. The (blue) pixels represent the number of detected ions: the darker the pixel the more ions it represents. The solid (red) line is the fit to the experimental data. Note that the averages include some non-resonant background as well as the resonant $^{34}Ar^{+}$ ions, which accounts for why the averages do not go through the densest concentration of pixels. See Sec. III B for more details.

revert to the conventional resonance procedure, for which we took the shape of the resonance curve from Ref. [13]. Very recently, the effects of ion-motion damping due to collisions with rest gas atoms have been incorporated into the function describing the Ramsey resonance shape [17]. Part of our data was checked with both fitting functions. No significant shifts were seen in the results so, for the analysis presented here, we used the function corresponding to the ideal lineshape.

C. Q_{EC} value determination

The $Q_{\rm EC}$ value is the total decay energy of the transition. It can be expressed as the difference between the mass of the parent atom $M_{\rm p}$ and that of the daughter $M_{\rm d}$:

$$Q_{\rm EC} = (M_{\rm p} - M_{\rm d})\, c^2. \qquad (3)$$

In terms of the measured cyclotron frequencies for the singly-charged ions of the parent and daughter, $\nu_{c,\rm p}$ and $\nu_{c,\rm d}$ respectively [see Eq. (2)], the $Q_{\rm EC}$ value can be written as

$$Q_{\rm EC} = \left(\frac{\nu_{c,\rm d}}{\nu_{c,\rm p}} - 1\right)(M_{\rm d} - m_e) + \Delta_{p,d}, \qquad (4)$$

where m_e is the electron rest mass and $\Delta_{p,d}$ arises from the atomic-electron binding-energy difference between the parent and daughter atoms. The latter contributes at most about 3 eV for the cases we report on here, since we studied only singly-charged ions.

D. Control of systematic errors

The $Q_{\rm EC}$ values reported in this work were all measured as parent-daughter doublets, both with the same value of A/q. Thus we can apply Eq. (4) to our results. Furthermore, we obtained the cyclotron frequency ratio by interleaving scans of the two ion species, about 30 s for one, then 30 s for the other, with the alternation repeated for a number of hours. The temporal drift of the magnetic field is of the order of 3×10^{-11} min^{-1} [18], so any shifts between one 30-s scan and the next would have made a negligible contribution to the frequency ratio.

We analyzed the data by splitting the alternating parent- and daughter-ion scans into approximately 30-minute intervals, each consisting of about 30 pairs of scans. The 30 scan-pairs were not merged to form just one resonance curve for each ion species but several, the data being split according to the number of ions recorded per bunch. This allowed us to test for possible shifts in the resonance frequency due to multiple ions being stored in the trap [19]. (Our procedures will be described more fully for each measured $Q_{\rm EC}$ value in Sec. III.) The time-of-flight resonance results obtained for each 30-minute interval were then fitted separately for both ion species to get a frequency ratio. The final frequency ratio for a particular doublet was obtained from the weighted average of its interval results.

As an example of the quality of results, Fig. 5 shows the individual cyclotron frequencies obtained for the ^{34}Ar-

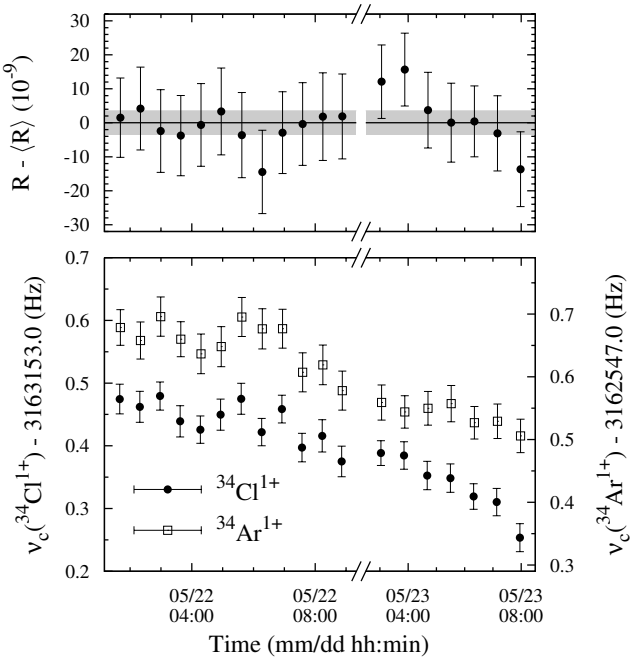

FIG. 5: A series of fitted cyclotron frequencies for ^{34}Ar and ^{34}Cl ions (lower panel). Each frequency point includes the results of 30 interleaved scans. The top panel shows the deviation of the corresponding frequency ratios, ν_d/ν_m from the average frequency ratio.

^{34}Cl pair, together with the deviations of the frequency ratios from the average value. It can be seen that, although the magnetic field fluctuates, the cyclotron-frequency ratios were consistent over an eight-hour period on one day, and a five-hour period a day later.

We have also considered other possible sources of systematic error. Tiny differences between the measured $\nu_+ + \nu_-$ and the actual cyclotron frequency ν_c could result from a slight misalignment of the electric- and magnetic-field axes, and from distortion in the quadrupole electric field [20]. Because the ion-pairs in our measurements are A/q doublets, the effect on the frequency ratio would be negligibly small compared to the statistical uncertainty. Mass-dependent shifts [21] are negligible as well, also because we are working with doublets having the same mass number. Previous measurements with JYFLTRAP have successfully reproduced accurately known isomeric excitation energies or $Q_{\rm EC}$ values [22, 23] down to a relative precision of $\Delta Q/M \approx 2 \times 10^{-9}$.

In the measurements reported here, by far the largest contribution to each final uncertainty is the statistical component, which originates from counting statistics and the fitting procedure.

III. RESULTS AND ANALYSIS

The $Q_{\rm EC}$ values of the superallowed β emitters ^{10}C, ^{34}Ar, ^{38}Ca and ^{46}V were all measured during a 9-day period of beam time in May 2010, only a month before the IGISOL and JYFLTRAP facilities were shut down in preparation for being moved to a different target location. Our four different frequency-ratio measurements are described individually in the following sections.

A. ^{10}C

The $Q_{\rm EC}$ value for ^{10}C proved to be the most difficult one we have measured so far. Mass-10 being the lightest mass ever measured with JYFLTRAP, we carefully tuned the setup before the on-line experiment began, using stable ^{10}B and ^{12}C ions from an off-line ion source. We found that the buffer-gas pressure of the purification Penning trap had to be significantly reduced since the cooling effect of the helium gas is much stronger for light ions. Even so, damping of the TOF-ICR resonance was rather pronounced and thus we could only use short excitation times. An additional difficulty was that the transmission of the RFQ was rather poor. Nevertheless, in the end enough ions could be delivered to the Penning trap for a successful measurement.

Unlike our experience with heavier ions ($A \geq 23$), a rather strong dipole component in the quadrupole field was apparent, as evidenced by a clear resonance observed at frequency ν_+, about 170 Hz away from the $\nu_+ + \nu_-$ sideband. This prevented our using Ramsey excitation, since the two resonance patterns overlapped. Instead, we used a conventional TOF-ICR resonance technique with a 200 ms excitation time.

Several checks of the data were done in order to ensure that the measurements yielded correct results despite the strong dipole component. In addition to measuring the $Q_{\rm EC}$ value between ^{10}C and ^{10}B, we also measured the well known mass of stable ^{13}C [26], using ^{12}C as the reference ion. Also, parameters like dipole-magnetron-excitation amplitude and ion-transfer time between the two traps were varied to check that there was no shift in the measured frequency ratio when the ions occupied a different fraction of the trap volume.

In all, we obtained seven sets of data for the ^{10}C $Q_{\rm EC}$ value and three for the ^{13}C mass. The data were analyzed using count-rate class analysis [19] to account for the effects of multiple stored ions in the trap. Moreover, to double-check our results, the class division was done in two different ways. In the first analysis, we subdivided the data into three classes according to how many ions were in each bunch, 1-2, 3 or 4-5. In the second analysis only two classes were retained, those with 1 ion/bunch and those with 2-3 ions/bunch. As can be seen from Fig. 6, the results from each group of 30 interleaved scans changed from one analysis to the other but the two average frequency ratios were consistent with one another. Our final frequency ratio and $Q_{\rm EC}$ value appear in Table II, and the latter is compared with previous measurements of the $Q_{\rm EC}$ value derived from (p,n) threshold measurements [27, 28] in Fig. 7.

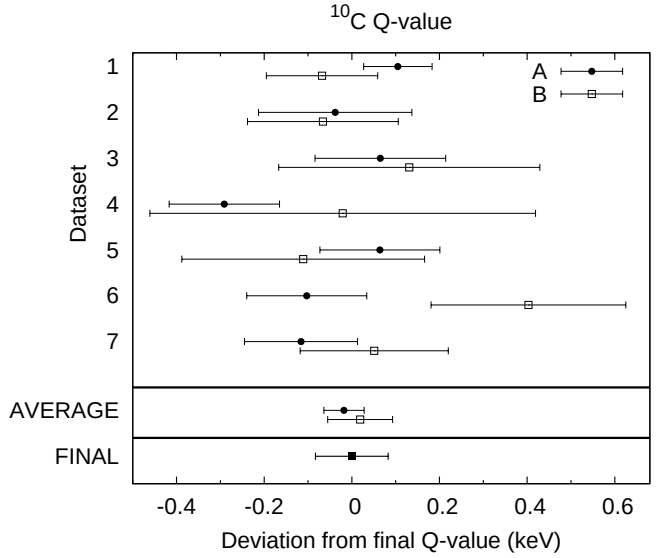

FIG. 6: $Q_{\rm EC}$ values obtained for each set of 30 scans. All the data were analyzed to account for multiple stored ions. In the data denoted by "A" the maximum number of ions per accepted bunch was 5, while those denoted "B" included a maximum of 3. We obtained the final value by taking the unweighted average of "A" and "B" and applying an error bar derived by taking the larger uncertainty of the two and adding the difference between "A" and "B" in quadrature.

TABLE II: The obtained frequency ratios and the derived $Q_{\rm EC}$ values or energy differences for ions having A=10, 34, 38 and 46.

Ion A	Ion B	Frequency ratio $\frac{\nu_B}{\nu_A}$	$Q_{\rm EC}$ or ΔE (keV)
Mass 10:			
^{10}C	^{10}B	1.000 391 157(9)	3648.12(8)
Mass 34:			
^{34}Ar	^{34}Cl	1.000 191 551 8(27)	6061.82(9)
^{34}Ar	^{34}Cl^m	1.000 186 923 2(33)	5915.37(10)
^{34}Cl^m	^{34}Cl	1.000 004 630(8)	146.52(26)
^{34}Ar	^{34}S	1.000 365 151(6)	11553.51(19)
Mass 38:			
^{38}Ca	^{38}K^m	1.000 186 955 0(28)	6612.15(10)
^{38}Ca	^{38}K	1.000 190 632 6(27)	6742.19(10)
^{38}K^m	^{38}K	1.000 003 681 5(38)	130.21(14)
^{38}Ca	^{38}Ar	1.000 357 913 2(32)	12656.36(11)
Mass 46:			
^{46}V	^{46}Ti	1.000 164 760 8(23)	7052.44(10)

The $Q_{\rm EC}$ value given in Table II is, of course, for the ground-state-to-ground-state transition. The superallowed transition feeds the 0^+ state in ^{10}B, which is at 1740.07(2) keV [2], so our result for the transition populating the ground state corresponds to a $Q_{\rm EC}$ value for the superallowed transition of 1908.05(8) keV.

Our control measurement of the ^{13}C-to-^{12}C mass difference yielded a frequency ratio of $\nu_c(^{12}\mathrm{C})/\nu_c(^{13}\mathrm{C}) = 1.083\,616\,728(5)$. This corresponds to a mass excess for ^{13}C of 3125.04(6) keV, which is in perfect agreement with the high-precision literature value of 3125.011(1) keV [26]. This further confirms that our ^{10}C $Q_{\rm EC}$ value does not suffer from any significant systematic error.

B. ^{34}Ar

To determine the $Q_{\rm EC}$ value for ^{34}Ar, we measured its frequency ratio, not only compared with ^{34}Cl but also with the high-spin (3^+) isomer ^{34}Cl^m and with its granddaughter ^{34}S. The two states in ^{34}Cl are only 146 keV apart, but were easily separated as we have done before [23] using the Ramsey cleaning method. The cyclotron frequencies were measured using a Ramsey-type excitation with the pattern 25/150/25 ms (on/off/on). This short excitation time was used because of the residual-gas impurities present in the precision trap. When we used longer times, we observed significant charge-exchange losses for all ion species. The effect of these losses is also evident in Fig. 4, where some ions are seen to appear at ≈170 μs time-of-flight regardless of the excitation frequency. This accounts for why the average time-of-flight points do not go through the darkest concentration of pixels in the figure: the contaminants, which appear at ≈170 μs and are probably singly charged O_2 molecules, serve to pull the average up a bit.

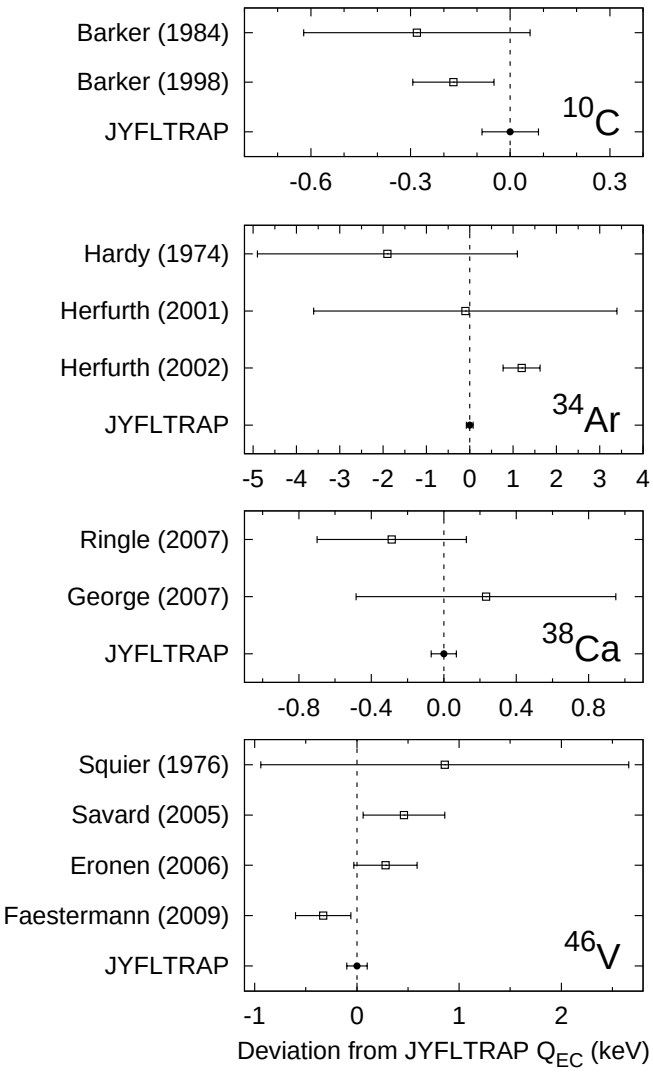

FIG. 7: Comparison of our $Q_{\rm EC}$ value measurements, labelled JYFLTRAP, with previous measurements. For each transition, our result is plotted at 0 on the abscissa, and the other results are plotted as differences $\left(Q_{\rm EC}^{\rm LIT.} - Q_{\rm EC}^{\rm JYFLTRAP}\right)$. The references from the top down are [27, 28, 30–32, 34–39] respectively.

To take this constant time-of-flight background into account, we added two additional fit parameters: a constant time of flight for the background, and the ratio of the number of background counts to that of the resonant ions. Despite the presence of contaminating ions, no systematic shifts of the fitted frequencies were observed as we increased the number of stored ions in the trap.

The frequency ratios and $Q_{\rm EC}$ values we obtained from these measurements are compiled in Table II and the final derived $Q_{\rm EC}$ values are in Table III. Our value for the excitation energy of the ^{34}Cl isomer, 146.52(26) keV, agrees well with our previous

JYFLTRAP value, 146.29(10) keV, which we reported in 2009 [23], and with a more precise value, 146.36(3) keV, obtained [29] from its decay γ ray. Furthermore, the three ^{34}Ar-^{34}Cl $Q_{\rm EC}$ values, derived via three different paths, are in remarkable agreement with one another. Our final result for the $Q_{\rm EC}$ value of this superallowed transition is 6061.83(8) keV.

This value is compared with previous measurements of the ^{34}Ar $Q_{\rm EC}$ value [30–32] in Fig. 7. The earliest of these results [30] was from a (p,n) Q-value measurement; the later two [31, 32] were Penning-trap measurements from ISOLTRAP. Only one of these results—the most recent value from ISOLTRAP[32]—has an uncertainty comparable to ours, although even its uncertainty is five times larger than ours. However, our result disagrees by three of the latter's standard deviations. We have no definitive explanation for this discrepancy but there is an important difference between the two measurements: ours obtained the ^{34}Ar $Q_{\rm EC}$ value directly by a measurement of the frequency ratio of the daughter to the parent ions. The ISOLTRAP measurement used ^{39}K as its reference ion. Thus, to get the ^{34}Ar $Q_{\rm EC}$ value, the mass of the daughter ^{34}Cl also had to be linked to ^{39}K. This link via ^{39}K – 5 mass units away – may well have been the source of error.

C. ^{38}Ca

Our measurement of the ^{38}Ca $Q_{\rm EC}$ value was conducted in the same way as the measurement just described for ^{34}Ar. The daughter nucleus in this case, ^{38}K, has a low-lying isomeric state just like ^{34}Cl has, although it is the isomeric state in ^{38}K that has spin and parity of 0^+ and the ground state that is 3^+. These states are only 130 keV apart but were easily separated with the Ramsey cleaning method. As with the ^{34}Ar measurement, we obtained the $Q_{\rm EC}$ value for ^{38}Ca, not only by a direct daughter-parent frequency ratio, but also via the high-spin ground state of ^{38}K and via the granddaughter nucleus ^{38}Ar. Charge-exchange background was evident in the ^{38}Ar frequency measurement but not for the other ion species. We used a Ramsey excitation pattern of 25/350/25 ms (on/off/on) for all measurements except for one set of data connecting ^{38}Ca to ^{38}Ar. In that case, we used a shorter excitation pattern, 25/150/25 ms, in order to confirm that there was no change in the results as the number of contaminant ions increased.

TABLE III: $Q_{\rm EC}$ values for the ^{34}Ar-to-^{34}Cl superallowed transition obtained via three different reference ions. The input data are taken from Table II and from Refs. [23, 29].

Method	$Q_{\rm EC}$ (keV)
^{34}Ar—^{34}Cl direct	6061.82(9)
via ^{34}Cl^m	6061.89(28)
via ^{34}S	6061.85(20)[a]
FINAL	**6061.83(8)**

[a]The mass difference between ^{34}Cl and ^{34}S [5491.662(47) keV] was taken from Ref. [23].

TABLE IV: $Q_{\rm EC}$ values for the ^{38}Ca-to-^{38}K^m superallowed transition obtained via three different reference ions. The input data are taken from Table II and from Ref. [23].

Method	$Q_{\rm EC}$ (keV)
^{38}Ca—^{38}K^m direct	6612.15(10)
via ^{38}K	6611.99(16)
via ^{38}Ar	6612.14(12)[a]
FINAL	**6612.12(7)**

[a]The mass difference between ^{38}K^m and ^{38}Ar [6044.223(41) keV] was taken from Ref. [23].

Our measured frequency ratios and $Q_{\rm EC}$ values appear in Table II and the final derived $Q_{\rm EC}$ values are in Table IV. Our measured value for the excitation energy of the ^{38}K isomer, 130.21(14) keV, agrees well with our previous JYFLTRAP value, 130.13(6) keV, and with the previously accepted value of 130.4(3) keV [33], which is the least precise. Furthermore, the three ^{38}Ca-^{38}K^m $Q_{\rm EC}$ values, derived via three different paths, are in excellent agreement with one another. Our final result for the $Q_{\rm EC}$ value of this superallowed transition is 6612.12(7) keV.

This value is compared in Fig. 7 with the two previous determinations of the ^{38}Ca $Q_{\rm EC}$ value, both based on Penning-trap mass measurements, one from the LEBIT trap [34] and the other from ISOLTRAP [35]. These two values, which are quite recent, and the new measured result we report here all agree within error bars. Our value, though, is about six times more precise than that in Ref. [34] and ten times more precise than Ref. [35].

D. ^{46}V

We have already measured the $Q_{\rm EC}$ value for the superallowed decay of ^{46}V once before at JYFLTRAP, in 2006 [38]. Our motivation for remeasuring it now was to improve the precision of the result. Since 2006 we have introduced a number of improvements to our system, most notably the rapid alternation of parent-daughter frequency scans and the use of Ramsey excitation. The excitation pattern used for this measurement was 25/350/25 ms (on/off/on). The resonances we obtained were clean and showed no evidence of any charge-exchange products. The frequency ratio and corresponding $Q_{\rm EC}$ value are presented in Table II.

Our new $Q_{\rm EC}$ value is compared with the four previous measurements of the ^{46}V $Q_{\rm EC}$ value [36–39] in Fig. 7. Our new result agrees with our previous one [38] but has an uncertainty smaller by a factor of three. In fact, our new result also agrees with the other three measurements, one of which is from the CPT Penning trap [37], another

TABLE V: The four $Q_{\rm EC}$ values for superallowed transitions that were obtained in this work. Also shown are the equivalent values quoted in the most recent survey of data [2] and the new weighted averages including our measurements.

		$Q_{\rm EC}$ values (keV)		
Parent	Daughter	this work	survey[2]	average
^{10}C	^{10}B(0^+)	1908.05(8)	1907.87(11)	1907.99(7)
^{34}Ar	^{34}Cl	6061.83(8)	6062.98(48)	6061.86(21)
^{38}Ca	^{38}K^m	6612.12(7)	6611.75(41)	6612.11(7)
^{46}V	^{46}Ti	7052.44(10)	7052.40(16)	7052.45(9)

is from a (^{3}He,t) reaction Q value [39], and the third is from a (p,n) threshold measurement [36]. All three have uncertainties at least a factor of three greater than our new result.

IV. CONCLUSIONS

Our four new $Q_{\rm EC}$-value results for superallowed transitions are collected in Table V, where they are compared with the equivalent values that appeared in the most recent survey of superallowed $0^+ \rightarrow 0^+$ nuclear β decay [2]. In all cases, our new results have reduced the uncertainties considerably, although in the case of ^{34}Ar the reduction is constrained by the inconsistency between our result and one of the previous measurements [32] (see Fig. 7). That inconsistency leads to a normalized χ^2 of 7 for the average and, following the procedures used in Ref. [2], we increase the uncertainty on the average by a scale factor equal to the square root of the normalized χ^2.

Although our improvement in $Q_{\rm EC}$-value precision for these four cases is significant, our results do not in themselves reduce the uncertainty in the corresponding $\mathcal{F}t$ values. For each case, the uncertainty in its $\mathcal{F}t$ value is dominated by another property of the transition: For ^{10}C, ^{34}Ar and ^{38}Ca, it is the branching ratio that dominates, while for ^{46}V it is the half-life. What our results do is to provide $Q_{\rm EC}$ values with fractional uncertainties that are comfortably below what is likely to be achieved in the near future for branching ratios or half-lives. Thus, whatever experimental improvements can be achieved in reducing the branching-ratio uncertainties for the decays of ^{10}C, ^{34}Ar and ^{38}Ca, that reduction will translate directly into reduced $\mathcal{F}t$-value uncertainties; and the same argument applies to the half-life of ^{46}V.

To give one example, the branching ratio for the superallowed transition from ^{34}Ar is currently known to a fractional uncertainty of 2.6×10^{-3} and its half-life to 4.7×10^{-4} [2]. The fractional uncertainty we report here for its $Q_{\rm EC}$ value is 1.3×10^{-5}, which corresponds to a fractional uncertainty on the statistical rate function f of 7.4×10^{-5}, a factor of six better than the half-life and a factor of 35 better than the branching ratio. Because ^{34}Ar has a rather favorable decay scheme, it should be possible with currently available techniques to reduce the branching-ratio uncertainty to 1.0×10^{-3} or even below that. This would lead to an $\mathcal{F}t$-value for ^{34}Ar at essentially that same precision. Then it would become possible for the first time to compare at the 0.1% level a mirror pair of superallowed transitions, ^{34}Ar$\rightarrow^{34}$Cl and ^{34}Cl$\rightarrow^{34}$S, a comparison that would help to distinguish among the various models used to calculate the isospin-symmetry-breaking correction to superallowed decays [4].

It is also interesting to note that our measurement has slightly increased the $Q_{\rm EC}$ value for the ^{10}C superallowed decay. If we take the average $Q_{\rm EC}$ value listed in Table V and include a new half-life measurement for ^{10}C [40] together with the data listed in the 2009 survey [2], we obtain an $\mathcal{F}t$ value for the ^{10}C superallowed transition of 3077.9(45) s. This is slightly outside error bars from the average of all $\mathcal{F}t$ values, 3072.08(79) s, obtained in the 2009 survey. If this discrepancy were to be confirmed by an improved branching-ratio value for ^{10}C and by a similarly high $\mathcal{F}t$ value for the ^{14}O decay, it could signal the appearance of a scalar current (see Ref. [2]). With this motivation, it is our plan in future to measure the $Q_{\rm EC}$-value of the superallowed transition from ^{14}O. Obviously, an improved value for the ^{10}C branching ratio would also be very welcome.

Acknowledgments

This work has been supported by the EU 6th Framework programme "Integrating Infrastructure Initiative-Transnational Access" Contract No. 506065 (EURONS) and by the Academy of Finland under the Finnish Centre of Excellence Programme 2006-2011 (Nuclear and Accelerator Based Physics Programme at JYFL). JCH was supported by the U. S. Department of Energy under Grant DE-FG03-93ER40773 and by the Robert A. Welch Foundation under Grant no. A-1397.

[1] I.S. Towner and J.C. Hardy, Rep. Prog. Phys. **73**, 046301 (2010).
[2] J. C. Hardy and I. S. Towner, Phys. Rev. C **79**, 055502 (2009).
[3] I.S. Towner and J.C. Hardy, Phys. Rev. C **77**, 025501 (2008).
[4] I.S. Towner and J.C. Hardy, Phys. Rev. C **82**, 065501 (2010)
[5] A. Jokinen *et al.*, Int. J. Mass Spectrom. **251**, 204 (2006).
[6] J. Äystö, Nucl. Phys. A **693**, 477 (2001).

[7] J. Huikari *et al.*, Nucl. Instrum. Methods Phys. Res., Sect. B **222**, 632 (2004).
[8] P. Karvonen *et al.*, Nucl. Instrum. Methods Phys. Res., Sect. B **266**, 4794 (2008).
[9] A. Nieminen *et al.*, Nucl. Instrum. Methods Phys. Res., Sect. A **469**, 244 (2001).
[10] G. Gräff, H. Kalinowsky, and J. Traut, Z. Phys. A **297**, 35 (1980).
[11] G. Savard *et al.*, Phys. Lett. A **158**, 247 (1991).
[12] T. Eronen *et al.*, Nucl. Instrum. Methods Phys. Res., Sect. B **266**, 4527 (2008).
[13] M. König *et al.*, Int. J. Mass Spectrom. **142**, 95 (1995).
[14] S. George *et al.*, Int. J. Mass Spectrom. **264**, 110 (2007).
[15] M. Kretzschmar, Int. J. Mass Spectrom. **264**, 122 (2007).
[16] K. Blaum *et al.*, J. Phys. B: At., Mol. Opt. Phys. **36**, 921 (2003).
[17] S. George *et al.*, Int. J. Mass Spectrom. **299**, 102 (2010).
[18] S. Rahaman *et al.*, Eur. Phys. J. A **34**, 5 (2007).
[19] A. Kellerbauer *et al.*, Eur. Phys. J. D **22**, 53 (2003).
[20] G. Gabrielse, Int. J. Mass Spectrom. **279**, 107 (2009).
[21] V.-V. Elomaa *et al.*, Nucl. Instrum. Methods Phys. Res., Sect. A **612**, 97 (2009).
[22] S. Rahaman *et al.*, Phys. Lett. B **662**, 111 (2008).
[23] T. Eronen *et al.*, Phys. Rev. Lett. **103**, 252501 (2009).
[24] P. H. Barker and S. M. Ferguson, Phys. Rev. C **38**, 1936 (1988).
[25] S. C. Baker, M. J. Brown, and P. H. Barker, Phys. Rev. C **40**, 940 (1989).
[26] G. Audi *et al.*, Nucl. Phys. **A729**, 327 (2003).
[27] P. H. Barker and R. E. White, Phys. Rev. C **29**, 1530 (1984).
[28] P. H. Barker and P. A. Amundsen, Phys. Rev. C **58**, 2571 (1998).
[29] K. A. Snover *et al.*, Phys. Rev. C **4**, 398 (1971).
[30] J. C. Hardy *et al.*, Phys. Rev. C **9**, 252 (1974).
[31] F. Herfurth *et al.*, Nucl. Instrum. Methods Phys. Res., Sect. A **469**, 254 (2001).
[32] F. Herfurth *et al.*, Eur. Phys. J. A **15**, 17 (2002).
[33] P.M. Endt, Nucl. Phys. A **521**, 1 (1990).
[34] R. Ringle *et al.*, Int. J. Mass Spectrom. **262**, 33 (2007).
[35] S. George *et al.*, Phys. Rev. Lett. **98**, 162501 (2007).
[36] G.T.A. Squier, W.E. Burcham, S.D. Hoath, J.M. Freeman, P.H. Barker and R.J. Petty, Phys. Lett. **65B**, 122 (1976).
[37] G. Savard *et al.*, Phys. Rev. Lett. **95**, 102501 (2005).
[38] T. Eronen *et al.*, Phys. Rev. Lett. **97**, 232501 (2006).
[39] T. Faestermann, R. Hertenberger, H.-F. Wirth, R. Krücken, M. Mahgoub and P. Maier-Komor, Eur. Phys. J. A, **42**, 339 (2009).
[40] P.H. Barker, K.K.H. Leung and A.P. Byrne, Phys. Rev. C 79, 024311 (2009).